Study on Frequency Stability of Magnetic Resonance Contactless Power Transmission System Based On PSSS Topology

Xin Zhao[1, a], Hai Fu Ye[1, b]

[1] Institute of Electronic Engineering, China Academy of Engineering Physics, Mianyang 621900, China

[a]zhaoxin881028@163.com, [b]yehaifu@126.com

Keywords: Wireless Power Transfer, Magnetic Resonance, Dynamic Resonance, Constant Frequency Control

Abstract. This paper, aimed at the magnetic resonance contactless power transmission system based on PSSS topology, analyzes the stability of the system resonant frequency when the load and the mutual inductance are changing and proposes the method of constant frequency control based on the technology of dynamic resonance and soft switching. The paper explains the operating principles of the proposal, builds the circuit model by using Simulink and conducts a simulation study.

Introduction

Compared to traditional inductive contactless power transmission technology, magnetic resonance contactless power transmission technology can generate a higher magnetic field so that the power can be transferred more efficiently at a farther distance. Magnetic resonance contactless power transmission technology is a kind of technology which is non-directional and can transfer several kilowatts of power efficiently at medium distance (The medium distance is more than a few times the diameter of the resonance coils) through non-metallic materials, having a relatively small effect on the human body and the environment [1]- [3].

Fig. 1 shows the schematic diagram of resonance contactless power transmission system based on PSSS topology. The coupling coils of the system consists of a transmitting coil, resonance coil 1, resonance coil 2 and a pick-up coil. C_p、 C_1、 C_2 and C_s are compensation capacitors which make the system work in resonant state by compensating the reactive power generated by the coupling coils. Therefore, to maximize the power transmission efficiency of the whole system, the inherent resonance frequency of each coupling coil must be consistent. However, the system load or coil mutual inductance can be affected by some factors in practical application, which makes the reflection impedance of the primary side change. In this way, the coupling coils are dissonant due to the inherent resonant frequency and the transmission power of the system is decreased[4,5].
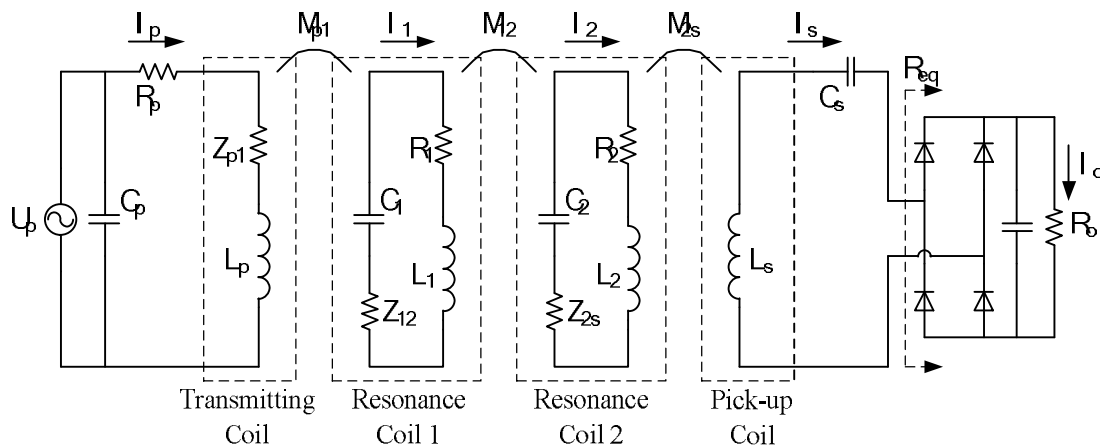

Fig. 1 The schematic diagram of resonance contactless power transmission system based on PSSS topology

In the case of the dissonance of the transmitting coil, the soft switching technology is usually adopted. But the characteristic of soft switch floating-frequency control can lead to the resonance coils

and the pick-up coil dissonance. Therefore, in the case of the dynamic change of the magnetic resonance system load or coil mutual inductance, the frequency of the system should be kept stable[6,7]. At present, the mainstream frequency stabilization control strategy is based on dynamic compensation, including dynamic capacitor compensation and phase control inductance. Dynamic capacitor compensation is limited by the dispersion of capacitive value, so the adjusting range is limited and the control is not easy to achieve; And a single control strategy based on phase control inductance is focused on tuning the inherent resonant frequency of resonant network, ignoring the power loss under the high frequency switching condition.

This paper, aimed at the magnetic resonance contactless power transmission system based on PSSS topology, analyzes the influence of system load and the coil mutual inductance on the inherent resonance frequency of system primary side, proposes a method of constant frequency control based on the technology of dynamic resonance and soft switching which achieves the stability of the inherent resonant frequency of coupling coils, and then builds the circuit model by using Simulink and conducts a simulation study.

The analysis of the resonance frequency of primary side

As shown in Fig. 1, U_p is the effective value of AC output voltage of high frequency inverter circuit, Z_{p1} is the equivalent reflection impedance from resonance coil L_1 to transmitting coil L_p, Z_{12} is the equivalent reflection impedance from resonance coil L_2 to resonance coil L_1, Z_{2s} is the equivalent reflection impedance from pick-up coil L_s to resonance coil L_2. And M_{p1} represents the mutual inductance between transmitting coil L_p and resonance coil L_1, M_{12} represents the mutual inductance between resonance coil L_1 and resonance coil L_2, M_{2s} represents the mutual inductance between resonance coil L_2 and pick-up coil L_s. In order to simplify the analysis, the radiation loss and the ohmic loss of the coils are ignored. According to the theory of mutual inductance, when all the coupling coils work in resonance state, equations can be obtained as follows:

$$
\begin{cases}
Z_{p1} = \dfrac{w_o^2 M_{p1}^2}{Z_{12}} \\[2mm]
Z_{12} = \dfrac{w_o^2 M_{12}^2}{Z_{2s}} \\[2mm]
Z_{2s} = \dfrac{w_o^2 M_{2s}^2}{R_{eq}} \\[2mm]
R_{eq} = \dfrac{8}{p^2} R_o \\[2mm]
C_p = \dfrac{L_p}{w_o^2 L_p^2 + Z_{p1}^2} \,.
\end{cases}
\tag{1}
$$

Then the following equation can be derived:

$$
\frac{p^4 w_p^4 M_{p1}^4 M_{2s}^4}{64 M_{12}^4 R_o^2} w_p^4 + L_p^2 w_p^2 - \frac{L_p}{C_p} = 0 \,.
\tag{2}
$$

Substituting the result of Eq. 2 to ω=2πf can give

$$
f_p = \sqrt{\frac{8 M_{12}^4 R_o^2 \left(\sqrt{L_p^4 + \dfrac{p^4 L_p M_{p1}^4 M_{2s}^4}{16 C_p M_{12}^4 R_o^2}} - L_p^2 \right)}{p^6 M_{p1}^4 M_{2s}^4}} \,.
\tag{3}
$$

And f_p is the inherent resonant frequency of transmitting coil resonant network.

In practical application, the relative position of transmitting coil L_p and resonance coil L_1 is fixed, so the mutual inductance M_{p1} can be regarded as a constant. Also, the mutual inductance M_{2s} can be regarded as a constant. Therefore, the paper will focus on the influence of changing mutual inductance M_{12} and system load R_o on f_p. As Eq. 3 shows, f_p will obviously change with the change of R_o and M_{12}. And they have a nonlinear relationship. Table 1 lists a set of parameters, where the change range of R_o is from 1.5Ω to 10Ω and the change range of M_{12} is from 0.05μH to 0.5μH.

Table 1 System Parameters

Parameters	Value
M_{p1}	0.61[μH]
M_{2s}	0.47[μH]
L_p	10[μH]
L_s	10[μH]
f	1[MHz]
R_o	2[Ω]
M_{12}	0.2[μH]

Substituting the parameters in Table 1 to Eq. 3, the relationship between f_p and M_{12} and R_o can be obtained, as shown in Fig. 2.
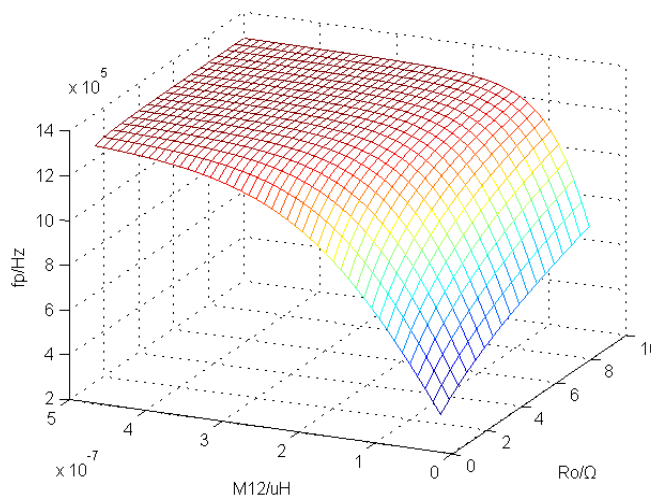

Fig. 2 The relation curve of f_p with M_{12} and R_o

Fig. 2 shows that f_p will change dramatically with the change of M_{12} and R_o in a certain range. Since the frequency of the magnetic resonance contactless power transmission system is usually a few MHz or even higher, even a small frequency drift can greatly attenuate the transmission power of the system. Appropriate control is needed to ensure the stability of the system's inherent resonant frequency.

Constant frequency control based on the technology of dynamic resonance and soft switching

The principle of dynamic resonance based on phase control inductance. The schematic diagram of the phase control inductance branch circuit is shown in Fig. 3, which consists of a fixed inductive Lt and two opposite switches S_{t1} and S_{t2}, and form the resonant compensation circuit of the primary side together with C_p. The circuit can change the conduction angle of Lt in the positive or negative half period by controlling S_{t1} and S_{t2} respectively to change the equivalent impedance of the resonant compensation circuit. Thus, the inherent resonance frequency of system primary side can be changed.
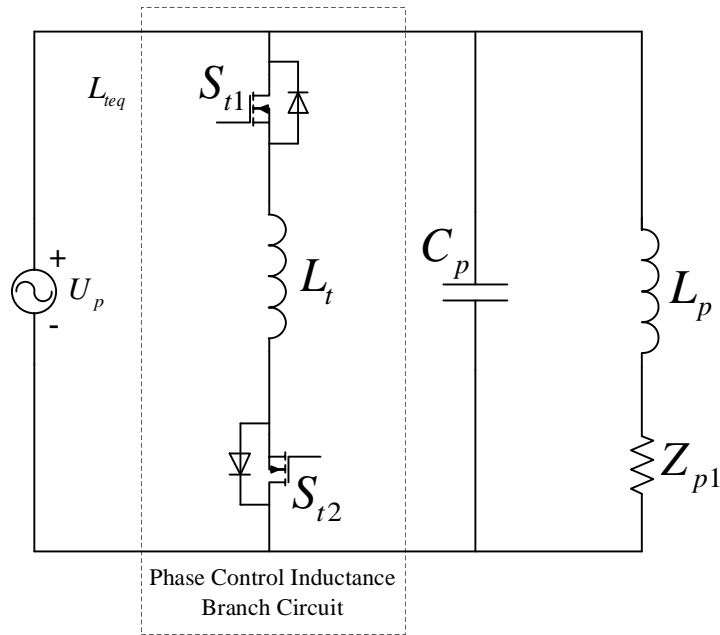
Fig. 3 The schematic diagram of phase control inductance branch circuit

As shown in Fig. 3, u_p is the input voltage of the circuit which is sinusoidal and defined as

$$u_p = \sqrt{2}U_p \sin(wt) , \tag{4}$$

where U_p is the effective value of the input voltage. Fig. 4 shows voltage and current waveform of L_t when internal resistance of L_t is ignored and $\alpha > \pi/2$ where α represents the trigger angle of switches. Since the energy stored by the inductor is equal to the energy released by it, the conduction angle of switches is $2\pi - 2\alpha$.
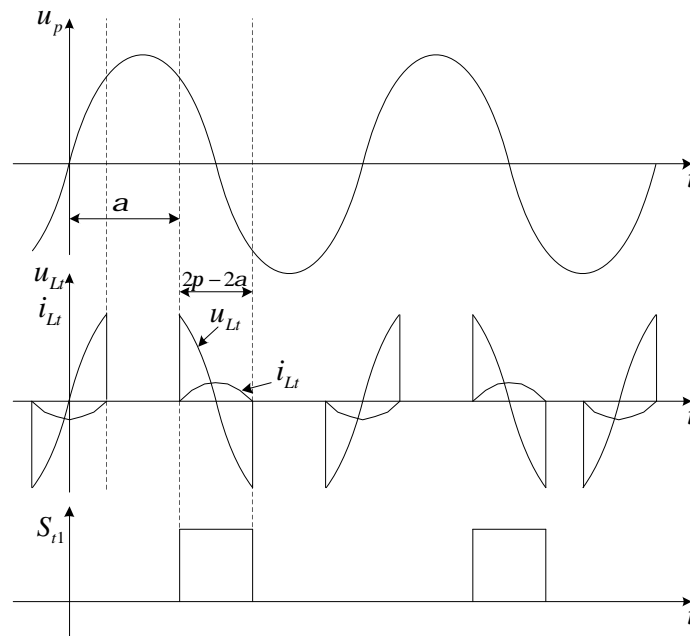

Fig. 4 The voltage and current waveform of L_t

By expanding the voltage of L_t with the form of Fourier series, U_{Lt}, which represents the fundamental component of the voltage of L_t, can be derived:

$$U_{Lt} = \frac{\sqrt{2}U_p}{p}(2p - 2a + \sin 2a)\cos wt . \tag{5}$$

And the effective values of U_{Lt} and the fundamental component of the current of L_t, represented by U_{LtRMS} and I_{LtRMS} respectively, are

$$\begin{cases} U_{LtRMS} = \dfrac{U_p}{p}(2p - 2a + \sin 2a) \\ I_{LtRMS} = \dfrac{U_{LtRMS}}{wL_t} \end{cases} \tag{6}$$

L_{teq} represents the equivalent inductance of the inductance phase controlling branch circuit. When the trigger angle is α, L_{teq} is

$$L_{teq} = \frac{U_p}{wI_{LtRMS}} = \frac{pL_t}{2p - 2a + \sin 2a} \tag{7}$$

According to Eq. 7, it can be obtained that, when the change range of α is from $\pi/2$ to π the variation range of L_{teq} is from L_t to infinity. That means it is available to adjust L_{teq} and change the equivalent impedance of the resonant compensation circuit by controlling α, thus to adjust f_p.

The principle of constant frequency control based on dynamic resonance. In order to realize the constant frequency control at the primary side of the system, the inductance phase controlling branch circuit is added to the schematic diagram shown in Fig. 1. The new circuit is shown in Fig. 5 after simplification.
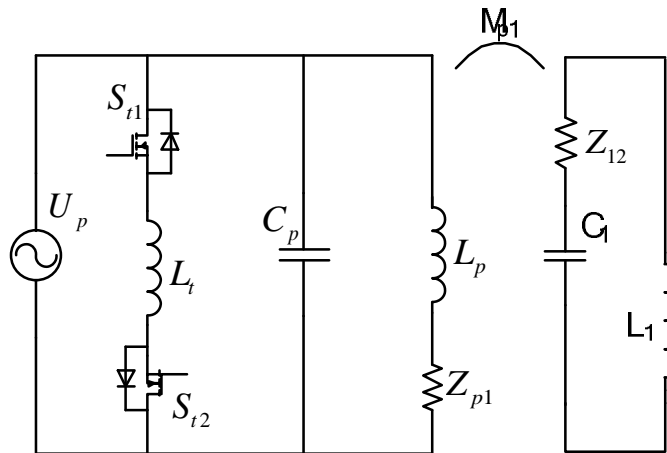

Fig. 5 Equivalent schematic diagram

According to Eq. 1, the following equation can be derived:

$$Z_{12} = \frac{8M_{12}^2 R_o}{p^2 M_{2s}^2} \tag{8}$$

Eq. 8 shows that both M_{12} and R_o changes will cause Z_{12} to change. Therefore, the dynamic resonance in the case of the change of M_{12} and R_o can be equivalent to the one in the case of the change of Z_{12}. Then Z_{12} represents the Varying load of the system shown in Fig. 5.

The admittance of the system shown in Fig. 5 is

$$G_P = \frac{1}{jw_o L_{teq}} + jw_o C_P + \frac{1}{jw_o L_p + Z_{p1}} \tag{9}$$

G_{p1} is the admittance of the primary side resonant network when L_t is not considered and can be calculated as

$$G_{P1} = jw_o C_P + \frac{1}{jw_o L_p + Z_{p1}} \tag{10}$$

where the static compensation capacitor C_p is

$$C_p = \frac{L_p}{w_o^2 L_p^2 + Z_{p1}^2} \tag{11}$$

Since dynamic resonance is based on inductance phase controlling, it is only when the equivalent impedance, after removing L_t, is capacitive when Z_{12} changes, the phase control inductance has the adjustable range of f_p. Set C_p as

$$C_p = C_{p1} = \frac{1}{w_o^2 L_p} = \frac{C_1 L_1}{L_p} \tag{12}$$

Im(G_{p1}) =0 can be obtained when the transmitting coil is in resonance. Substituting Im(G_{p1}) =0 to Eq. 12 can give

$$L_{teq} = \frac{1}{w_o^2 C_{p1} - \dfrac{w_o^2 L_p}{Z_{p1}^2 + w_o^2 L_p^2}} = \frac{1}{w_o^2 C_{p1} - \dfrac{L_p}{\dfrac{w_o^2 M_{p1}^4}{Z_{12}^2} + L_p^2}} \tag{13}$$

According to Eq. 1, the relation curve of L_{teq} with Z_{12} can be derived as shown in Fig. 6, which shows that the relationship of L_{teq} and Z_{12} is monotonous. This shows that when the system is in constant frequency control, in the case of Z_{12} changes, L_{teq} can be adjusted dynamically to keep Im(G_{p1}) =0 valid, thus to keep the inherent resonance frequency of primary side stable.
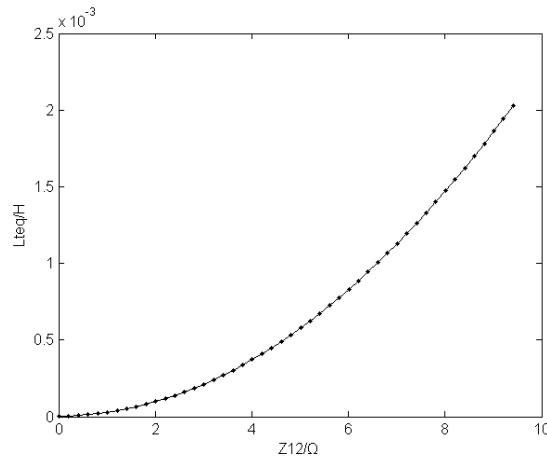

Fig. 6 The relation curve of L_{teq} with Z_{12}

According to Eq. 13, when Z_{12} approaches zero L_{teq} has a minimum as follows:

$$L_{teq(min)} = \lim_{Z_{12} \to 0} \frac{1}{w_o^2 C_{p1} - \dfrac{L_p}{\dfrac{w_o^2 M_{p1}^4}{Z_{12}^2} + L_p^2}} = \frac{1}{w_o^2 C_{p1}} = L_p \tag{14}$$

When Z_{12} approaches infinity L_{teq} has a maximum as follows:

$$L_{teq(max)} = \lim_{Z_{12} \to \infty} \frac{1}{w_o^2 C_{p1} - \dfrac{L_p}{\dfrac{w_o^2 M_{p1}^4}{Z_{12}^2} + L_p^2}} = \infty \tag{15}$$

According to Eq. 14 and Eq. 15, when Z_{12} ranges from 0 to infinity, L_{teq} ranges from L_p to infinity. According to the previous conclusion, when α ranges from $\pi/2$ to π, L_{teq} ranges from L_t to infinity. Therefore, to make sure there is always a α to keep Im(G_{p1}) =0 valid when Z_{12} changes, the value range of phase control inductance should be:

$$L_t \leq L_{teq(\min)} = L_p \tag{16}$$

Constant frequency control strategy based on soft switch technology. The function of the dynamic resonance branch circuit is to make the inherent resonance frequency of primary side consistent with the system operating frequency by adjusting the L_{teq} to change inherent resonance frequency when they are different. Based on this, this paper proposes a constant frequency control strategy based on soft switch technology. To be more specific, a high frequency inverter controlled by soft switch is adopted at primary side of system to track and sample f_p, and then to generate corresponding controlling signals to adjust the L_{teq} to make the inherent resonance frequency of primary side consistent with the system operating frequency by comparing the sample frequency and the rated operating frequency of system. Thus, when M_{12} and R_o change, the system can work stably at resonance frequency, and the high frequency inverter of primary side controlled by soft switch is achieved to reduce switch loss at the same time.

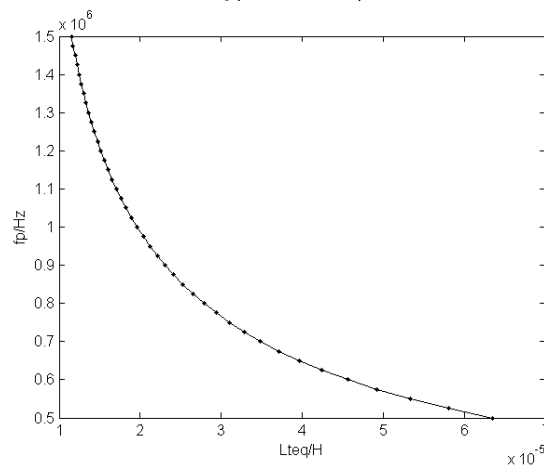According to Eq. 13, the relation curve of f_p with L_{teq} can be derived as shown in Fig. 7

Fig. 7 The relation curve of f_p with L_{teq}

According to Eq. 7, Eq. 13 and Fig. 7, the following control logic can be obtained:

(1) When $f=f_p>f_o$, increase L_{teq} to increase α ;

(2) When $f=f_p<f_o$, decrease L_{teq} to decrease α ;

(3) When $f=f_p=f_o$, just keep α constant.

When the system is under constant frequency control, the waveform of U_p, drive voltage of the high frequency inverter circuit and drive voltage of the inductance phase controlling branch circuit are shown in Fig. 8.
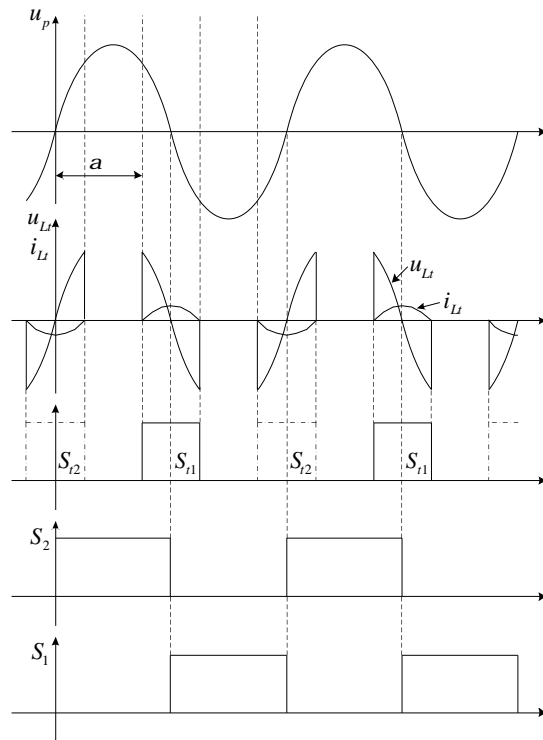
Fig. 8 The waveform of U_p, drive voltage of the high frequency inverter circuit
and drive voltage of the inductance phase controlling branch circuit

Since circuit is not ideal in practice, when switch S_{t1} or S_{t2} shut off, the current in the circuit may not reduce to zero, the stray inductance will produce a high reverse voltage the moment the switch shut off, which may lead to damage of the switch. Therefore, it is necessary to extend the turn-on time of switch S_{t1} and S_{t2} to make the duty cycle of the switch drive waveform rise to 50%, thus, to make the two drive waveform complementary, so that switch S_{t1} and S_{t2} work in zero current switching(ZCS) mode, as shown in Fig. 9.
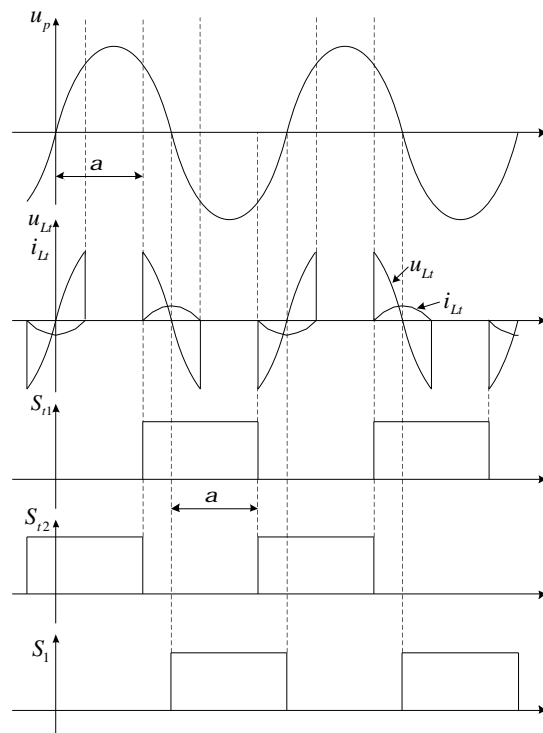

Fig. 9 The waveform of U_p, drive voltage of the high frequency inverter circuit
and drive voltage of the inductance phase controlling branch circuit after improvement

Simulation Study

Build the circuit model by using Simulink. Fig. 10 shows the schematic diagram of simulation circuit under constant frequency control, where the high frequency inverter circuit is a push-pull full bridge inverter circuit, Z_{12} represents the varying load when M_{12} and R_o change. Table 2 lists the main parameters of the simulation.
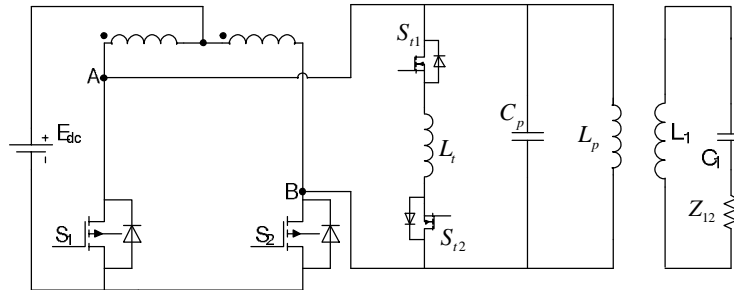

Fig. 10The schematic diagram of simulation circuit under constant frequency control

Table 2 Simulation Parameters

Parameters	Value
M_{p1}	0.45[μH]
L_t	5[μH]
L_p	5[μH]
L_1	10[μH]
C_p	6[μF]
C_1	5.0661[μF]
f	1[MHz]
Z_{12}	10,2[Ω]

The simulation time is 0.001s. In the simulation process, the system firstly works in hard-switching mode with the rated working frequency f_o; then works in soft-switching mode at 0.0003s, that is floating frequency control. And the system starts constant frequency control at 0.0004s. Z_{12} is adjusted from 10Ω to 2Ω at 0.0007s and then the simulation is ended in 0.001s. Fig. 11, Fig. 12 and Fig. 13 show the results of the simulation. Fig. 11 shows the change of system working frequency during the whole simulation process. Fig. 12 and Fig. 13 show respectively the drive voltage waveform of the high frequency inverter circuit, the voltage waveform of the primary resonant network, the voltage and current waveform of phase control inductance and the voltage and current waveform of load when Z_{12} is 10Ω and 2Ω after the system starts constant frequency control.
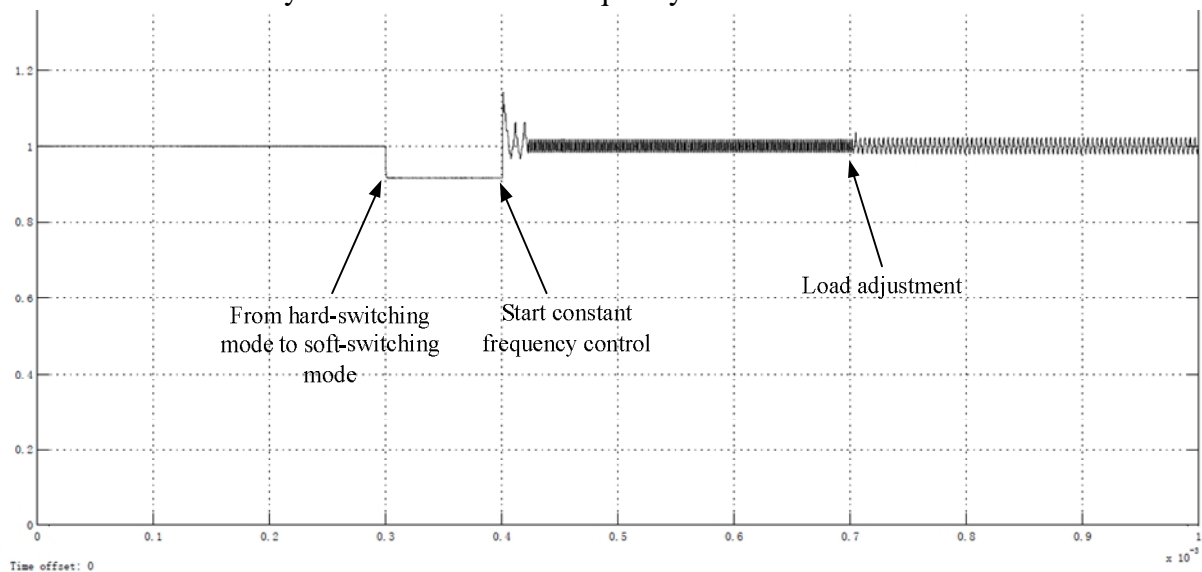

Fig. 11 The change of system working frequency during the whole simulation process
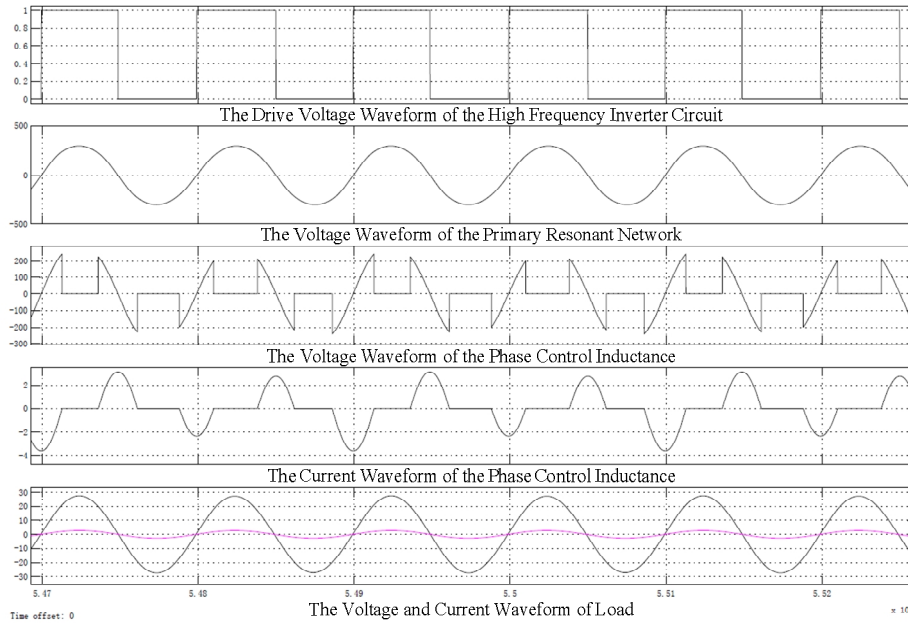
Fig. 12 The drive voltage waveform of the high frequency inverter circuit, the voltage waveform of the primary resonant network, the voltage and current waveform of phase control inductance and the voltage and current waveform of load when Z_{12} is 10Ω
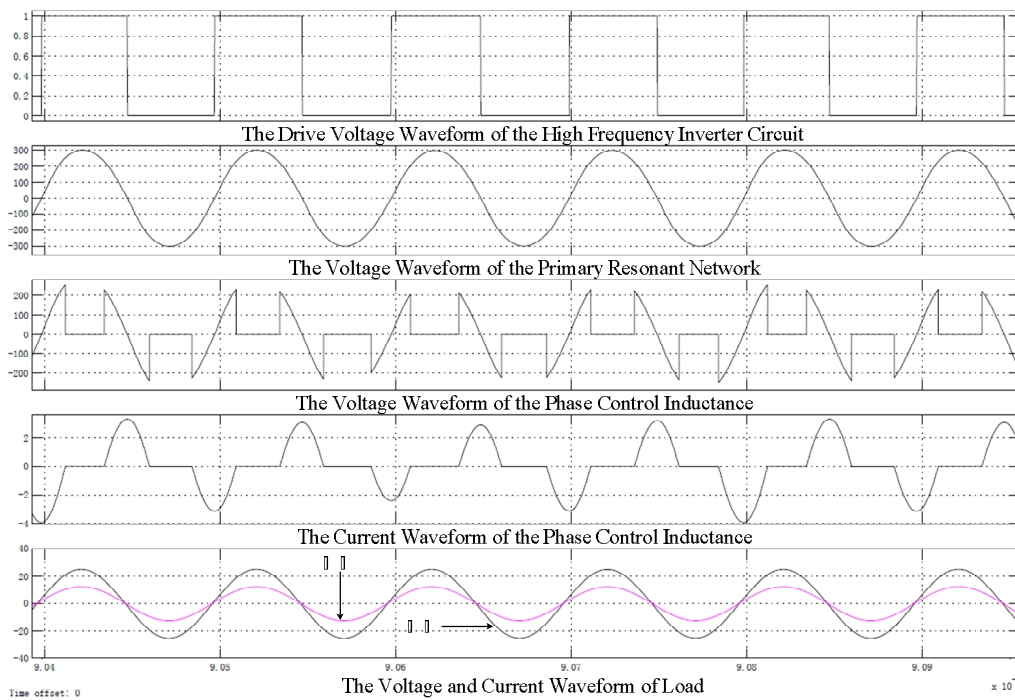

Fig. 13 The drive voltage waveform of the high frequency inverter circuit, the voltage waveform of the primary resonant network, the voltage and current waveform of phase control inductance and the voltage and current waveform of load when Z_{12} is 2Ω

From the simulation results it can be concluded that when Z_{12} changes, the system can work stably at resonance frequency, and the high frequency inverter of primary side works in zero voltage switching (ZVS) mode at the same time.

Conclusion

This paper, aimed at the magnetic resonance contactless power transmission system based on PSSS topology, analyzes the influence of system load and the coil mutual inductance on the inherent

resonance frequency of system primary side, proposes the constant frequency control strategy based on dynamic resonance and soft switching technology which achieves the stability of the inherent resonant frequency, and then builds the circuit model by using Simulink and conducts a simulation study. The simulation results show that the constant frequency control strategy is feasible.

References

[1] Boys J T, Hu A P, Covic G A. Critical Q Analysis of a Current-fed Resonant Converter for ICPT Applications[J]. Electronics Letters, 2000, 36(17): 1440-1442.

[2] André Kurs, Aristeidis Karalis, Robert Moffatt, et al. Wireless Power Transfer via Strongly Coupled Magnetic Resonances[J]. Science, 2007, 317(5834): 83 – 86.

[3] Yuan Zhai. Study on Optimization and Control of Magnetic Resonance Mode Wireless Power Supply System[D]. Chongqing University. 2013.

[4] Yu Gang Su, Chun Sen Tang, Yue Sun, Zhi Hui Wang. Load Adaptive Technology of Contactless Power Transfer System[J]. Transaction of China Electrotechnical Society, 2009, 24(1): 153-157.

[5] Chen Yang Xia. Research on Analysis and Optimization for Transmission Power and Efficiency of Inductively Coupled Power Transfer System[D]. Chongqing University. 2010.

[6] Chun Sen Tang, Yue Sun, Yu Gang Su, et al. Determining multiple steady-state ZCS operating points of a switch-mode contactless power transfer system [J]. IEEE Transactions On Power Electronics, 2009, 24(2): 416–425.

[7] Chwei-Sen Wang, Grant A. Covic, Oskar H. Stielau. Power Transfer Capability and Bifurcation Phenomena of Loosely Coupled Inductive Power Transfer Systems [J]. IEEE Transactions On Power Electronics, 2004, 51(1): 148-157.